



OPEN DDTC-Cu(I) inhibits human osteosarcoma cells growth by repressing MET/PI3K/AKT signaling pathway

Ruhao Zhou^{1,2,4}, Lei Yan^{1,2,4}, Kun Zhang^{1,2}, Song Chen^{1,2}, Yang Yu^{1,2}, Xiaochun Wei^{1,2}, Yongchun Pan³, Chaojian Xu^{1,2}, Xiaojuan Sun^{1,2}, Zhi Lv^{1,2}, Pengcui Li^{1,2}, Xiaochen Qiao^{1,2}, Yi Feng^{1,2}✉ & Zhi Tian^{1,2}✉

Osteosarcoma (OS) is a frequently occurring bone malignancy with increased metastatic properties, causing deaths in large numbers around the world. Disulfiram (DSF) is clinically utilized to treat alcohol dependency and has been indicated to bind Cu(I) in-vivo to form DDTC-Cu(I), which has been confirmed for its antitumor effects. This investigation aimed to elucidate the efficacy of DDTC-Cu(I) on OS cell apoptosis, migration, growth, invasion, and underlying mechanisms. The in-vitro investigations were performed on U2OS, SaOS2, and MG-63 OS cell lines and included CCK-8, colony formation, RTCA, transwell invasion, flow cytometry, wound healing, and RNA seq assays. DDTC-Cu(I) was inoculated dose-dependent, increased apoptosis, and suppressed cells' ability to proliferate, migrate, and invade via the MET and PI3K/AKT signaling pathways. Additionally, MET's overexpression partially reversed the anti-OS and PI3K/AKT signaling pathways suppression effect of DDTC-Cu(I). Furthermore, the SaOS2 xenograft mice model was utilized to confirm the in-vivo anti-OS efficacy of DDTC-Cu(I) by MET protein inhibition. The histological research revealed that DDTC-Cu(I) had no adverse influence on the liver, heart, lungs, and kidneys. Overall, the data of this investigation suggested that DDTC-Cu(I) could serve as an efficient agent against OS development.

Keywords Disulfiram, DDTC-Cu(I), Osteosarcoma, RNA seq, MET/PI3K/Akt signaling pathway

Osteosarcoma (OS) is the most frequently occurring malignant bone tumor with a high incidence of tubular long bones metaphysis, specifically in adolescents and teenagers' proximal tibia, distal femur, and humerus. 1.7–4.4 per million are affected by OS with increased metastatic and invasive capacity¹. The OS progression leads to disability and death, causing marked psychological and financial burdens. In individuals with localized, non-metastasis OS, after the neoadjuvant chemotherapy, surgical resection, and adjuvant chemotherapy, the event-free 5-year survival rate is about 60–70%². However, at initial diagnosis, most patients indicate metastasis, usually in the lung, and have a substandard prognosis and 20–30% of 5-year survival rate even after standard therapeutic strategies^{3,4}. Because of the limitation of conventional treatment strategies, novel therapies with the potential to improve the overall survival of OS are urgently required.

Disulfiram (DSF) is a clinical drug utilized for treating alcohol deterrents in the USA⁵. In-vivo, DSF is rapidly converted to its reduced metabolite-DDTC. DDTC is generally thought to combine with copper (Cu) to perform antitumor effects⁶. Jonathan B. Mandell et al. indicated that DSF, doxorubicin, and Cu are efficient treatment strategies and should be taken to early-phase trials for treating metastatic sarcoma patients and refractory diseases⁷. Furthermore, DSF/Cu markedly inhibits OS cell growth, causing death by autophagy, cell arrest, and apoptosis via the ROS/JNK signaling pathway activation⁸. The stomach and the small intestines substantially absorb Cu, which then binds albumin, is transported to the liver via portal blood, and transmitted to peripheral tissues after attaching with ceruloplasmin or albumin (to a lesser extent). Cu enters the cells via different

¹Second Clinical Medical College, Shanxi Medical University, 382 Wuyi Road, Taiyuan 030001, Shanxi, People's Republic of China. ²Department of Orthopedics, Shanxi Key laboratory of Bone and Soft Tissue Injury Repair, The Second Hospital of Shanxi Medical University, 382 Wuyi Road, Taiyuan 030001, Shanxi, People's Republic of China. ³Department of Orthopedics, The Third People's Hospital of Datong City, Datong 037006, Shanxi, People's Republic of China. ⁴Ruhao Zhou and Lei Yan contributed equally to this work. ✉email: fengyi160@126.com; drtianzhi@163.com

transmembrane transporters, and Cu(II) is reduced to Cu(I)⁹. Han et al. revealed that DDTC-Cu(I) is generated using DDTC (a DSF monomer), Cu chloride, and sodium sulfite (Supplementary Fig. 1). And DDTC-Cu(I) can substantially inhibit in-vitro pancreatic cancer cell proliferation and in-vivo tumor growth¹⁰.

Therefore, this investigation elucidated if DDTC-Cu(I) has an anti-OS effect are indicated that DDTC-Cu(I) can suppress OS cell invasion, growth, migration, and tumorigenesis. Furthermore, MET/PI3K/AKT signaling pathway was studied to elucidate the underlying DDTC-Cu(I) mechanisms of anti-proliferation effects on OS.

Materials and methods

Cell culture

The human OS cell lines (SaOS2, MG63, and U2OS) were acquired from ATCC and propagated at 37 °C in Dulbecco's modified Eagle's medium (DMEM) augmented with antibiotics and fetal bovine serum (FBS, 10%) in 5% CO₂ humidified incubator.

Cell transfection

The plasmids pcDNA3.1-MET and its negative control pcDNA3.1-NC (the empty transfection control plasmid pcDNA3.1) were provided by the Public Protein/Plasmid Library (China) and were transfected into SaOS2 cells via Lipofectamine 3000 Reagent (Invitrogen). The transfected were propagated in 6-well plates for 48 h for future experiments.

Chemical synthesis

For in-vivo and in-vitro analyses, DDTC-Cu(I) complex was prepared at 1 mmol/L concentration equal to the molar quantity of DDTC or Cu (all DDTC-Cu(I) concentrations were equal to the molar quantity of Cu or DDTC). First, Cu chloride dehydrates, sodium diethyldithiocarbamate trihydrate, and sodium sulfite (Sigma-Aldrich, Shanghai, China) were solubilized in sterilized water to form a 200 mmol/L concentration. In the second step, sodium diethyldithiocarbamate (50 μL), sodium sulfite (25 μL), and Cu chloride (50 μL) were prepared as the first step using sterilized water (9 mL) by gentle mixing. The third step included the addition of sterilized water in the prepared solution to a total volume of 10 mL. Lastly, the prepared solution was packed and stored at 4 °C.

Cell proliferation assay

The cell count kit-8 (CCK-8, MedChemExpress, New Jersey, USA) was utilized to elucidate the viability of OS cells, per the kit's guide. Briefly, 5×10^3 cells/100 μl medium were propagated in a 96-well plate and treated with different reagents. Then 100 μl of CCK-8 detection solution (90 μl fresh medium + 10 μl CCK-8 reagent) was added to the cells and incubated for 2 h at 37 °C and 5% CO₂. After 2 h, optical density was evaluated via a microplate reader (Biotek, Winooski, VT, USA) at 450 nm. The real-time cell analysis (RTCA) was performed to assess DDTC-Cu(I) treated OS cell viability. The CO₂ incubator is equipped with an xCELLigence RTCA analyzer, with the control RTCA software (ACEA Biosciences; USA) outside. To elucidate the real-time cytotoxic response, 16-well microplates (E-plates; Roche Diagnostics) were used for propagating SaOS2 and U2OS cells at 5.0×10^3 /well density. Impedance was measured every 15 min. After 20 h incubation, DDTC-Cu(I) in 0, 0.1, 0.2, 0.4, 0.8, 1.6, 3.2, and 6.4 μM concentrations were inoculated in the cultures of 200 μL, respectively, at 24, 48, and 72 h. RTCA-DP software (Roche Diagnostics GmbH) was utilized for cell viability.

Cloning formation assay

The OS cells were trypsinized and propagated for 24 h in a 6-well plate (500 cells/well). Then, different DDTC-Cu(I) concentrations were added to the cells for another 24 h. After the drug treatment, the media was refreshed every 2 days by DMEM with 10% FBS. After 6 days, the cells were preserved for 20 min using 4% paraformaldehyde (PFA) and dyed for 30 min with 1% crystal violet. Two investigators captured clone images and quantified those comprising > 50 cells via microscopic. The protocol was repeated thrice.

Wound healing assays

The OS cells were propagated in a 6-well plate until full confluency. Cells were scratched using a sterile pipette tip through the wells' center to create wounds. Then with the help of PBS, cells were washed and treated with DDTC-Cu(I) (0, 0.5, or 1 μM) in DMEM. The wounds were photographed and assessed at specific time points via Image J software (National Institutes of Health). The migration rate = (0 h scratch width - end time scratch width) / 0 h scratch width × 100%. The protocol was repeated thrice.

Transwell invasion assay

The invasion ability of cells was assessed using 24-well chamber plates with upper chambers' 8-μm porous membrane laminated with Matrigel matrix. The Matrigel Matrix Reduced (180 μl, Corning, NY, US) was diluted with the serum-free medium in 1:3 to coat 24-well inserts for 2 h. Then SaOS2 and U2OS (1×10^6 cells/mL) after 24 h pretreatment with different concentrations of DDTC-Cu(I) in 200 μl of DMEM containing 1% FBS was added to the upper chambers. 600 μL of DMEM with 10% FBS was inoculated in the basolateral chambers. After 72 h incubation in 5% CO₂ and 37 °C, the remaining upper membrane cells were removed using cotton swabs, and those which invaded across the membrane were rinsed twice, preserved for 15 min with 4% PFA, dyed for 15 min using 0.5% crystal violet, and quantified from 5 images/well.

Flow cytometry analysis of cell apoptosis

After treatment with different DDTC-Cu(I) doses for 24 h, SaOS2, and U2OS were harvested for flow cytometric assay. Cells were washed using cold PBS and preserved overnight in pre-cold 70% ethanol at 4 °C for the cell cycle distribution experiment. Briefly, cells were stained with propidium iodide (PI) for 30 min at 37 °C in

the dark. Per the manufacturer's guide, the cell apoptosis assay was carried out by PE Annexin V Apoptosis Detection Kit I (BD Biosciences, USA). After 7-Amino-Actinomycin (7-AAD) and PE Annexin V staining for 15 min at ambient temperature, the cell apoptosis rate was assessed via the flow cytometer. Cells that indicated negative 7-AAD and positive PE Annexin V were in the early apoptotic phase, while double-positive cells were either in late apoptosis or dead.

RNA-seq and data analysis

Whole RNA was acquired with the help of the TRIzol reagent (Invitrogen, CA, USA) per the kits' protocol. The NanoDrop 2000 spectrophotometer (Thermo Scientific, USA) assessed the purity and quantity of RNA, whereas its integrity was evaluated via the Agilent 2100 Bioanalyzer (Agilent Technologies, Santa Clara, CA, USA). The libraries were prepared with the help of the VAHTS Universal V6 RNA-seq Library Prep Kit per kits' method. OE Biotech Co., Ltd. (Shanghai, China) carried out the transcriptome sequencing and assessment.

Western blot analysis

Whole cellular protein was acquired by RIPA lysis buffer augmented with a protease/phosphorylase inhibitor cocktail (Keygen, Nanjing, China). The obtained protein was quantified via bicinchoninic acid (BCA) and separated in 10% SDS-PAGE gels, transplanted on a polyvinylidene difluoride membrane (Millipore, Danvers, MA, USA), which were then labeled with anti-c-MET (1:1000, ab51067, Abcam, Cambridge, UK), anti-PI3K (1:1000, A0982, ABclonal, Wuhan, China), anti-p-PI3K (1: 1,000, #4228, CST, MA, USA), anti-AKT (1:1000, A17909, ABclonal, Wuhan, China), anti-p-AKT (1:1000, AP0140, ABclonal, Wuhan, China), and GAPDH (1:12000, AP0063, Bioworld Technology, Nanjing, China) antibodies. The membrane immunoblots were developed using the enhanced chemiluminescence reagent, and band intensity was assessed by densitometric analysis via IMAGEJ software for relative protein levels quantification. The tumor β -actin was utilized for protein normalization.

In-vivo assessment

BALB/c is nude ($n=21$, female, age=5 w) mice were acquired from the Charles River Laboratory (Beijing, China) and were subcutaneously implanted with SaOS2 cells ($1 \times 10^6/200\mu\text{L}$) + Matrigel (200 μL) into the back flank^{11,12}. The mice were housed in an SPF "barrier" facility and, after 2 weeks of implantation, were randomly categorized into 3 treatment groups ($n=7/\text{group}$), including (1) control: received dexamethasone (0.5 mg/kg), (2) low concentration treatment: received DDTC-Cu(I) (5 nmol/g) and dexamethasone (0.5 mg/kg), and (3) high concentration treatment: received DDTC-Cu(I) (10 nmol/g) and dexamethasone (0.5 mg/kg). All the treatments were given intra-peritoneally (i.p.)/day (QOD). The 1 mmol/L DDTC-Cu(I) concentration was utilized. Tumor size was assessed every 2 days, and tumor volume (V) was measured as described in our previous research (8 CCL). After the treatment lasted 14 days, the mice were euthanized with isoflurane and samples from the heart, tumors, liver, kidneys and lungs were collected. The tumors were weighed and photographed. All specimens were preserved with 4% PFA for hematoxylin and eosin (H&E) staining and immunohistochemistry experiments.

Histopathology and immunohistochemistry

The specimens (the heart, tumors, liver, kidney, and lungs) were submerged in paraffin, sliced (4 μm thick), dewaxed, and stained with H&E Staining Kit (Beyotime Biotechnology, China) per the manufacturer's instructions¹³. Furthermore, their protein levels in OS xenografts were elucidated by using the sliced tumor samples for immunohistochemistry using Ki67 (A2094, Abclonal, Wuhan, China) or c-Met (ab51067, Abcam, Cambridge, UK) primary antibodies and a horseradish peroxidase-tagged goat anti-mouse IgG (ZSGB-BIO, Beijing, China).

Statistical measurement

The data are depicted as mean \pm SD of at least three experimental replicates and assessed via SPSS 21.0 (IBM, Chicago, IL, USA) and GraphPad Prism 6 software. The inter-group significant differences were elucidated using a two-tailed Student's t-test, whereas one-way ANOVA was performed to analyze the statistical significance between three or more groups. $P < 0.05$ was termed statistically essential.

Ethics statement

The study was conducted in accordance with the ARRIVE guidelines¹⁴ and all procedures were performed in accordance with institutional guidelines for animal research and were approved by the local committee at the Second Hospital of Shanxi Medical University (approval number DW2022054).

Results

DDTC-Cu(I) suppresses in-vitro osteosarcoma cell proliferation

hFOB1.19, U2OS, SaOS2, and MG-63 cells were treated with increasing DDTC-Cu(I) doses, and then their viability was elucidated at 24, 48, and 72 h via CCK-8 assay. DDTC-Cu(I) was administered to hFOB1.19 osteoblasts to assess its safety. The results showed that DDTC-Cu(I) below 1.6 μM for 24 h did not cause significant damage to normal cells (Figs. 1A). And it was revealed that DDTC-Cu(I) inhibited cellular functions in time- and concentration-dependent manner (Figs. 1B, C and D), with 24-hour IC_{50} values as 0.81, 0.63, and 1.35 μM , respectively (Fig. 1E). At 0.5 μM concentration, DDTC-Cu(I) more efficiently inhibited all cell lines proliferation than its precursors, DDTC, CuCl_2 , and Na_2SO_3 (Fig. 1F). Furthermore, the RTCA assay showed a concentration-dependent decrease in cell survival index after treatment with DDTC-Cu(I) (Fig. 2A, B). Compared with control cells, SaOS2 and USOS treated with DDTC-Cu(I) exhibited fewer colonies (Fig. 2C, D).

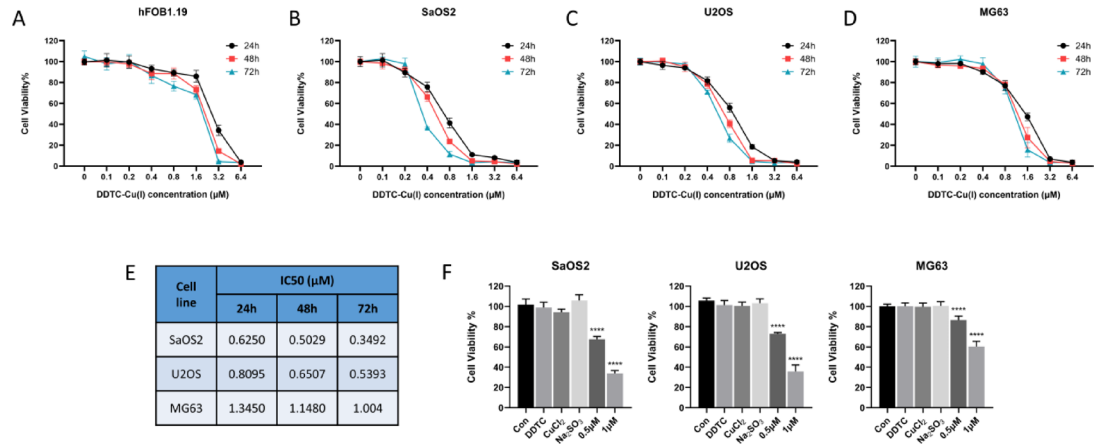


Fig. 1. (A–D) hFOB1.19, SaOS2, U2OS and MG63 cell lines were treated with incremental concentrations of DDTC-Cu(I) for 24, 48, and 72 h, respectively. (E) IC50 values were calculated and shown in a table. (F) SaOS2, U2OS and MG63 cell lines were treated with sterile saline, DDTC, CuCl₂, Na₂SO₃, 0.5 μM of DDTC-Cu(I) and 1 μM of DDTC-Cu(I) for 24 h. (The data are depicted as mean ± SD of at least three experimental replicates. *P* < 0.05 was termed statistically essential, **p* < 0.05, ***p* < 0.01, ****p* < 0.001, *****p* < 0.0001 vs. the control group)

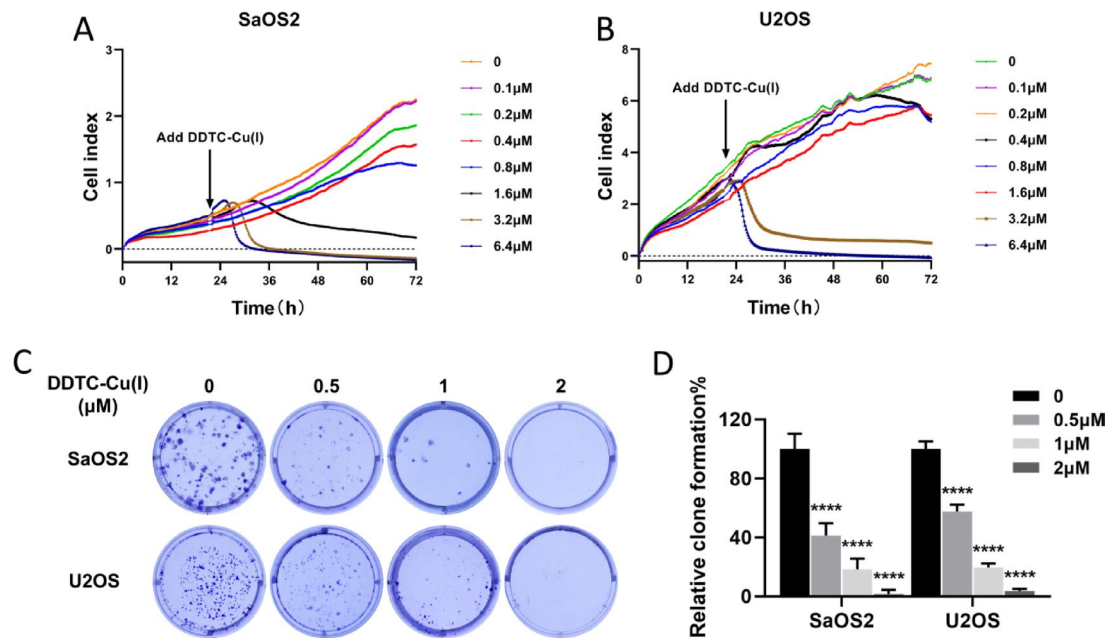


Fig. 2. (A–B) SaOS2 and U2OS cells were treated with incremental concentrations of DDTC-Cu(I) for 0–72 h, respectively. An RTCA assay was used to determine the cell viability. (C–D) SaOS2 and U2OS cells were inoculated in six-well plates and treated with 0, 0.5, 1, and 2 μM DDTC-Cu(I), respectively. After 6 days of incubation, colony formation was evaluated by crystal violet staining. (The data are depicted as mean ± SD of at least three experimental replicates. *P* < 0.05 was termed statistically essential, **p* < 0.05, ***p* < 0.01, ****p* < 0.001, *****p* < 0.0001 vs. the control group).

DDTC-Cu(I) inhibits osteosarcoma cells' ability to migrate and invade

The ability to migrate and invade is crucial for distant OS metastasis and local invasion. To elucidate if DDTC-Cu(I) repressed these abilities of SaOS2 and U2OS cells, wound healing and Matrigel-coated Transwell experiments were performed to identify the effect of DDTC-Cu(I) on migration and invasion. It was indicated that the healing rate CAR treatment group scratch was markedly decreased than the control group (Fig. 3A–D), indicating that DDTC-Cu(I) may suppress cell migration ability. Furthermore, the Matrigel-coated Transwell revealed that the number of OS cells that crossed the chamber membrane was reduced after DDTC-Cu(I) treatment (Fig. 3E–G), suggesting that DDTC-Cu(I) could also inhibit invasion activity.

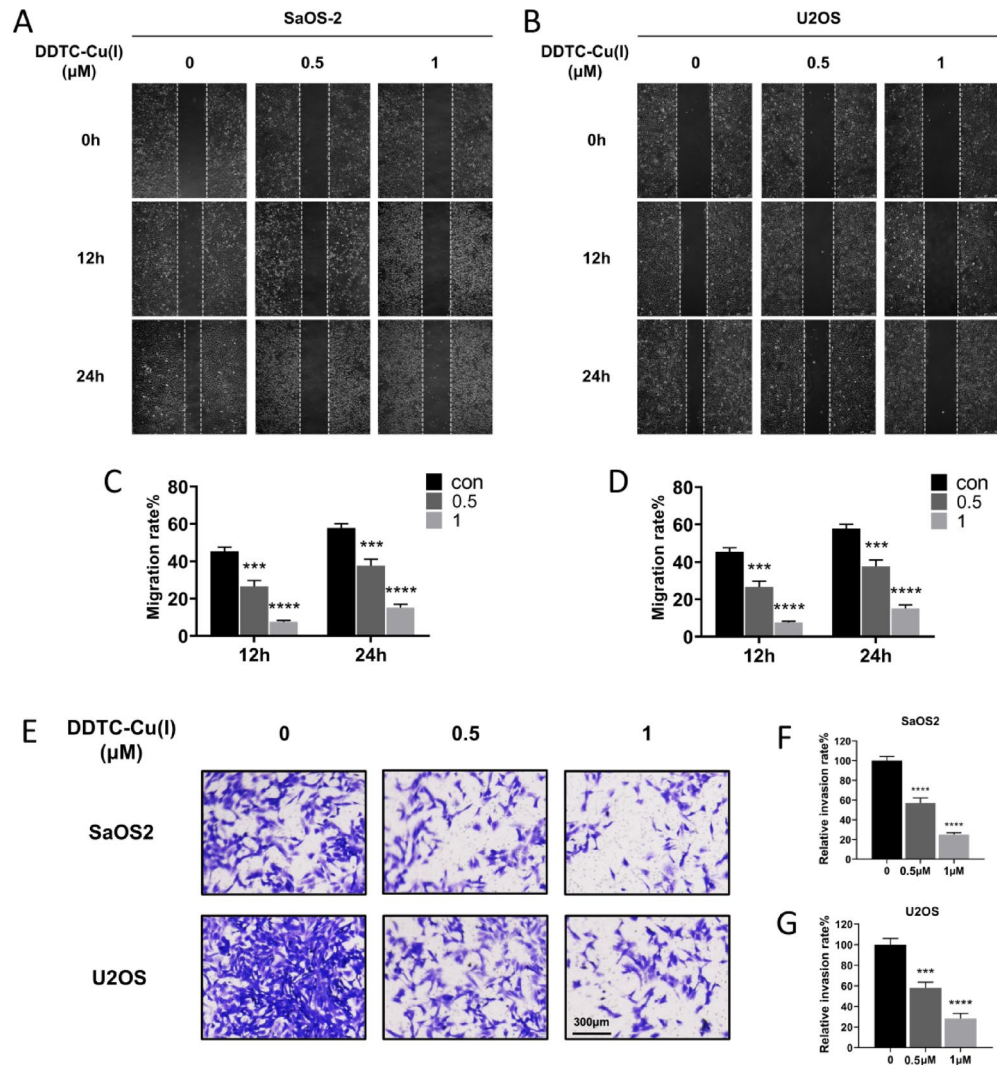


Fig. 3. (A–D) SaOS2 and U2OS cells were seeded, scratched and incubated with different concentrations of DDTC-Cu(I) for 12 / 24 h. Migration rates were measured by Fiji-4.0.1. Scale bar, 500 μ m. (E–G) Representative images of transwell invasion assays in SaOS2 and U2OS. Manual methods were used to quantify invaded cells. Scale bar, 300 μ m. SaOS2 and U2OS cells were preprocessed with 0 / 0.5 / 1 μ M of DDTC-Cu(I) for 24 h. (The data are depicted as mean \pm SD of at least three experimental replicates. $P < 0.05$ was termed statistically essential, * $p < 0.05$, ** $p < 0.01$, *** $p < 0.001$, **** $p < 0.0001$ vs. the control group).

DDTC-Cu(I) promotes osteosarcoma cells' apoptosis

To verify if DDTC-Cu(I) affects the OS cells' apoptosis, flow cytometry was performed to assess the apoptotic rate of U2OS and SaOS2 cells, which revealed that a markedly increased percentage of apoptosis after DDTC-Cu(I) treatment (Fig. 4A, B).

DDTC-Cu(I) regulates osteosarcoma cells' MET/PI3K/AKT signaling pathways

To delineate the mechanism of DDTC-Cu(I) in OS, transcriptome sequencing was carried out to evaluate the alterations in mRNA of DDTC-Cu(I) treated cells. Many differentially expressed genes (DEGs) were identified (Fig. 5A and B), coincidentally consistent with the previously studied MET (Fig. 5B), inhibited by DDTC-Cu(I). The Kyoto Encyclopedia of Genes and Genomes (KEGG) pathway assay indicated that these DEGs were notably enriched in the PI3K/AKT pathway (Fig. 5C). Furthermore, Western blotting confirmed the RNA-seq results that c-MET, PIK3CB, p-PIK3CB, AKT, and p-AKT protein expression was downregulated (Fig. 5D). DDTC-Cu(I) exerted anti-OS effects by suppressing MET and PI3K/AKT signaling pathways.

Overexpression of MET reverses the suppression of DDTC-Cu(I) in osteosarcoma cells

To further explore the MET functions, it was overexpressed to elucidate the PI3K/AKT pathway inhibition and MET expression. In Fig. 6E, MET protein (c-MET) overexpression was indicated in the pcDNA3.1-MET group than in the pcDNA3.1-NC group (the empty transfection control plasmid pcDNA3.1). Moreover, it was revealed that MET overexpression could partially rescue the suppression of OS cells' ability to proliferate, migrate, and

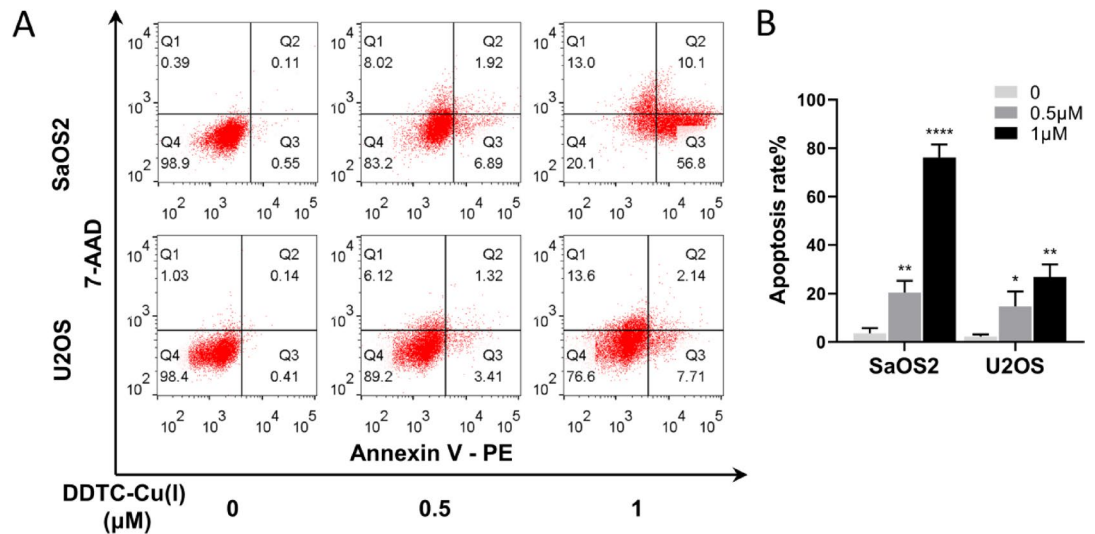


Fig. 4. (A) The effect of 0.5 / 1 μM of DDTC-Cu(I) on apoptosis of SaOS2 and U2OS cells was analyzed by flow cytometer. The bottom left quadrant shows clusters of viable cells (Q2), the bottom right quadrant shows the early apoptotic cells (Q3), and the top right quadrant shows the late apoptotic cells (Q4). (B) The quantification analysis (The data are depicted as mean \pm SD of at least three experimental replicates. $P < 0.05$ was termed statistically essential, * $p < 0.05$, ** $p < 0.01$, *** $p < 0.001$, **** $p < 0.0001$ vs. the control group).

invade after DDTC-Cu(I) (Fig. 6A–C) and promote apoptosis (Fig. 6D). Comparing the pcDNA3.1-MET(+) and the pcDNA3.1-NC(+) groups, MET overexpression markedly upregulated p-PIK3CB, AKT, and p-AKT protein expression. Moreover, MET overexpression could reverse the suppression of DDTC-Cu(I) on the PI3K-AKT pathway in OS cells by comparing the pcDNA3.1-MET(+)-DDTC-Cu(I)(+) group to the pcDNA3.1-NC(+)-DDTC-Cu(I)(+) group. Therefore, it is suggested that DDTC-Cu(I) might have an anti-OS agent by inhibiting MET and, thus, the PI3K/AKT signaling pathway.

DDTC-Cu(I) inhibits in-vivo osteosarcoma cell tumor growth

A xenograft model was established to validate the in-vivo anti-OS property of DDTC-Cu(I). DDTC-Cu(I) was revealed to suppress OS growth dose-dependently (Fig. 7A, B). Compared to the control group, the volume, and weight of xenograft tumors substantially reduced in DDTC-Cu(I)-treated mice (Fig. 7C, D). Mouse body weights were not significantly different between the three groups (Fig. 7E). Moreover, the in-vitro results were consistent with IHC staining, which indicated that DDTC-Cu(I) suppresses the level of c-MET and Ki67 (Fig. 8A). Moreover, H&E staining revealed no discernable pathologic alterations in the major mice organs of different groups (Fig. 8B). Altogether, this data further validated that DDTC-Cu(I) inhibits in-vivo OS tumor growth.

Discussion

The OS patients' prognosis improved after therapy. However, despite researchers' hard work and efforts in the last four decades, the OS survival rates are still unsatisfactory, specifically in individuals with local relapse or systemic metastasis^{15,16}. This investigation is the 1st to indicate the in-vitro and in-vivo anti-OS impact of DDTC-Cu(I). Here, the underlying anti-tumor mechanism of DDTC-Cu(I) was elucidated. Differential gene, KEGG pathway^{17–19} and western blot analyses revealed that DDTC-Cu(I) inhibits OS cells' ability to proliferate, invade, and migrate via MET/PI3K/AKT pathway.

c-MET, a hepatocyte growth factor (HGF) receptor, was first identified in OS cells exposed to carcinogens²⁰. Our previous investigation also found that MET is essential for the development and progression of OS. In cancers, MET is either overexpressed or mutated, for instance, in cervical, non-small-cell lung, and gastrointestinal cancers, and is essentially for cancer progression and is involved in tumor cell scattering, proliferation, and cell invasion²¹ representing an attractive target for tumor therapy^{22–24}. However, the association of the MET signaling pathway in OS, the most common primary bone malignancy, is poorly studied. Comprehensive MET gene research has indicated that MET oncogene is essentially linked with OS initiation and advancement, and a few of its inhibitors were proven effective for treating OS^{25,26}. Fioramonti et al. indicated that cabozantinib, a c-Met inhibitor, influences OS growth by directly affecting tumor cells and bone microenvironment modifications²⁷. Sampson et al. revealed that in the xenograft model, MET inhibitor PF-2,341,066 suppresses OS growth and osteolysis/matrix production²⁸.

Here, it was indicated that DDTC-Cu(I) could repress MET expression, suppress the OS cells' ability to proliferate, migrate, and invade and stimulate apoptosis.

In cancer researches, evidences have demonstrated that the PI3K-AKT signaling pathway is regulated by c-MET^{29–31} including osteosarcoma³². Wang et al. revealed that c-Met inhibition suppresses the PI3K/AKT pathway, enhancing cisplatin chemosensitivity²². Furthermore, the PI3K/AKT signaling pathway can be

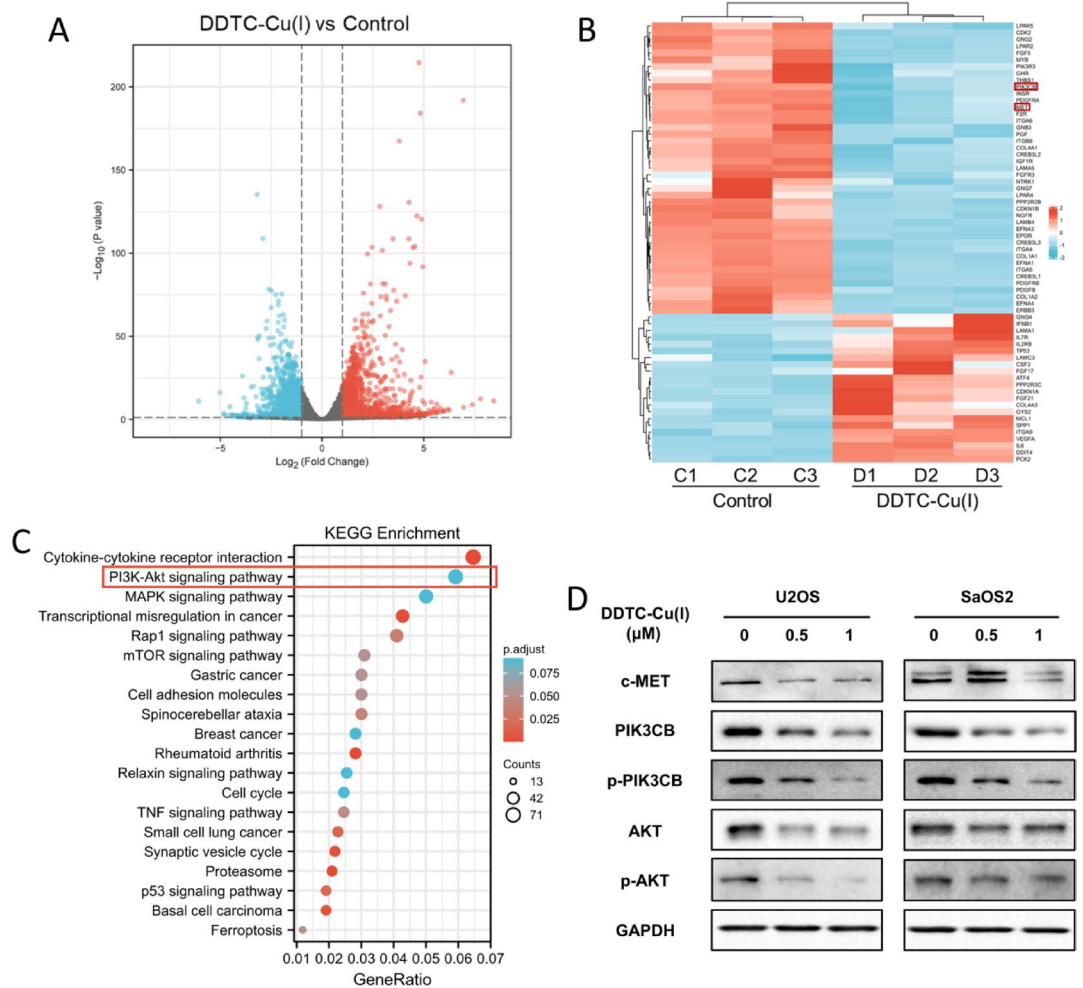


Fig. 5. (A–B) SaOS2 cells were treated with for DDTC-Cu(I) 24 h, and then the cells were subjected to RNA-seq analysis to identify differentially expressed genes. (C) KEGG pathway enrichment. (D) Western blot analysis revealed changes in the expression of c-MET and critical molecules in the PI3K/AKT signaling pathway in SaOS2 and U2OS cells.

suppressed by targeting MET reduction to alleviate OS cells' malignancy in-vitro³³. The PI3K/AKT pathway is one of human cancer's most important oncogenic pathways³⁴. There is mounting evidence suggesting that in OS, the PI3K/AKT pathway is frequently hyperactivated and promotes disease initiation and development processes, such as proliferation, tumorigenesis, cell cycle progression, invasion, inhibition of apoptosis, metastasis, angiogenesis, and chemoresistance^{35–38}.

In our study, we not only found that DDTC-Cu(I) could inhibit the expression of MET and PI3K/AKT signaling pathway and inhibit the progression of OS, but our results also indicated that the efficacy of DDTC-Cu(I), including the inhibitory effect on OS progression and the reduction of PI3K/AKT, could be partially rescued by overexpression of MET. Therefore, we suggest that DDTC-Cu(I) may exert an inhibitory effect on OS by inhibiting the MET/PI3K/AKT signaling pathway.

In summary, per our knowledge, this is the 1st investigation that elucidates the anti-tumor impact of DDTC-Cu(I) on OS in-vitro and in-vivo, suggesting its anti-OS activity, without significant cytotoxicity. Furthermore, it was mechanistically indicated that DDTC-Cu(I) exerted anti-OS impact via MET/PI3K/AKT signaling pathway. Altogether, this research confirms the anti-OS effect of DDTC-Cu(I) on OS, furnishing a new thought for the clinical treatment of OS.

Conclusion

The DSF, an alcohol withdrawal drug, forms DDTC-Cu(I) in-vivo after binding with Cu(I) and suppresses OS progression in U2OS, SaOS2, and MG63 cells and the SaOS2 xenograft mice model. Moreover, OS cells' ability to proliferate, invade, migrate, and metastasize was inhibited, and apoptosis was induced via MET/PI3K/AKT pathways suppression, validated in human OS cell SaOS2 xenograft mice. Altogether, it was suggested that DDTC-Cu(I) could be a valuable new anti-OS therapy. Additionally, efficient clinical trials are required to validate our understanding of the pharmacological effects and antitumor therapy of DDTC-Cu(I) in OS.

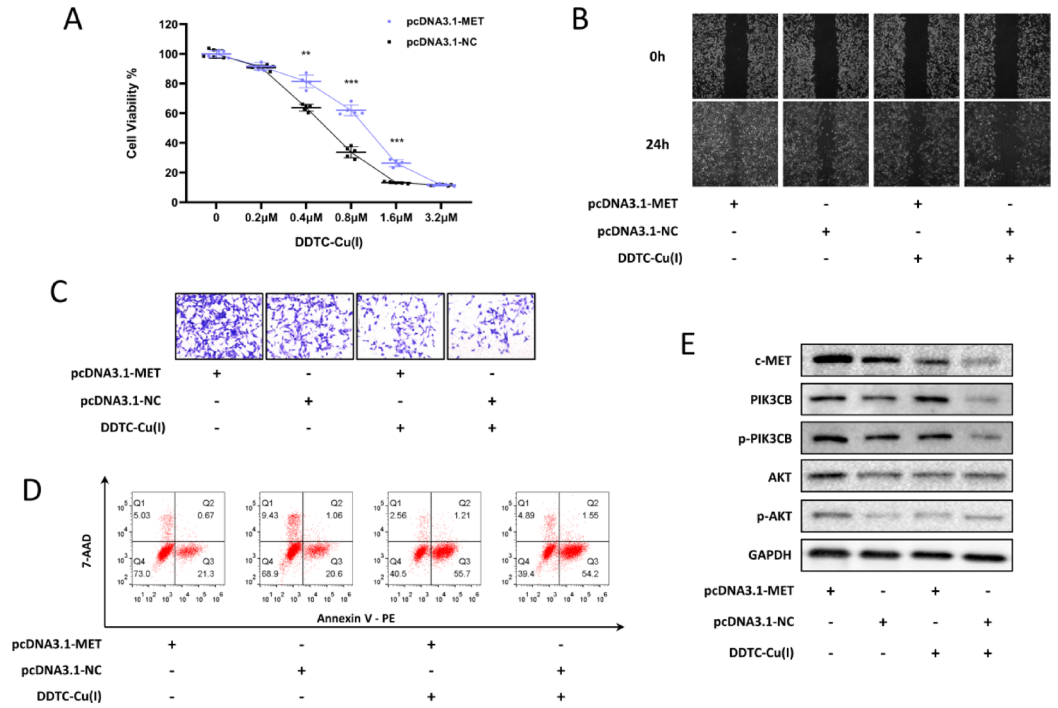


Fig. 6. (A) SaOS2 cells overexpressing MET and negative control (NC, the empty transfection control plasmid pcDNA3.1) were treated with different concentrations of DDTC-Cu(I) for 24 h, respectively, and cell viability was detected by CCK-8. (B) SaOS2 cells overexpressing MET and NC were seeded, scratched and incubated with 0 / 0.5 μM of DDTC-Cu(I) for 24 h. Migration rates were measured by Fiji-4.0.1. Scale bar, 500 μm. (C) SaOS2 cells overexpressing MET and NC were preprocessed with 0 / 0.5 μM of DDTC-Cu(I) for 24 h, followed by transwell assay. (D) After treated with 0 / 0.5 μM of DDTC-Cu(I) for 24 h, SaOS2 cells overexpressing MET and NC was analyzed by flow cytometer. (E) Western blot analysis revealed changes in the expression of c-MET and critical molecules in the PI3K/AKT signaling pathway in SaOS2 cells overexpressing MET and NC treated with 0/0.5 μM of DDTC-Cu(I).

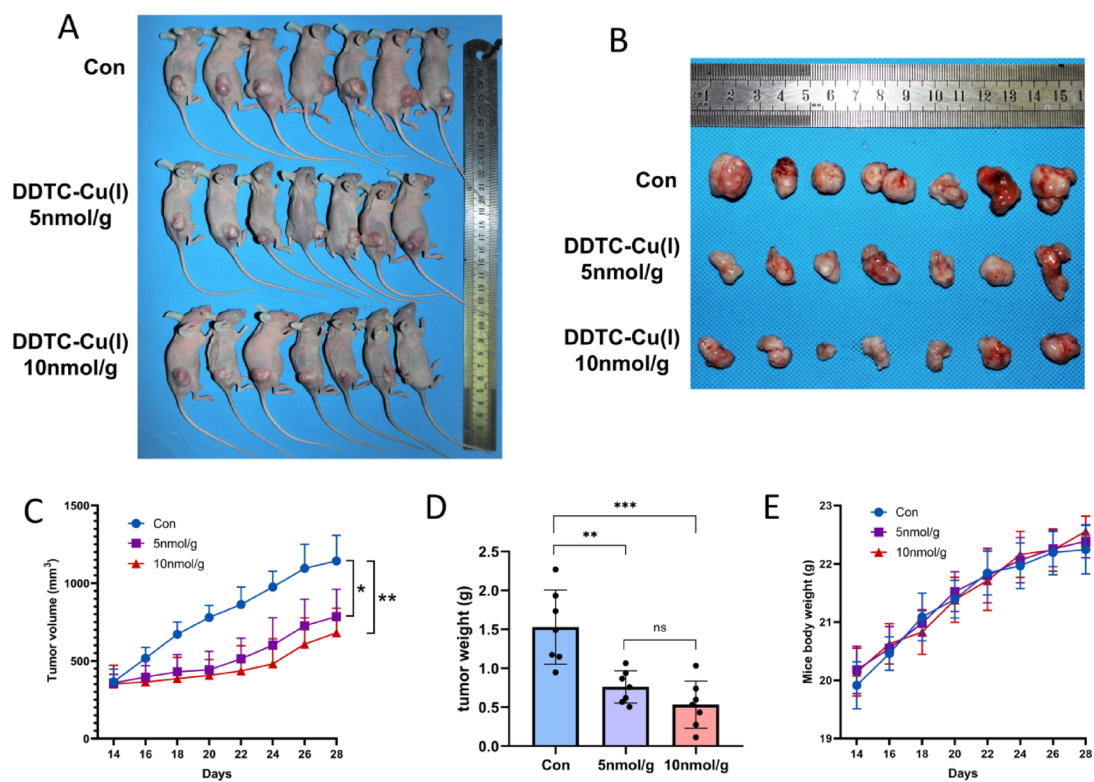


Fig. 7. (A) OS mice after treatment with different concentrations of DDTC-Cu(I). (B) The volumes of excised OS samples in each group. (C) The evolution of tumors volumes over time in each group. (D) Weight of excised OS samples in each group. (E) Mice body weights in each group. Statistics using one-way ANOVA with Tukey's test. The data represent means \pm SD. * $p < 0.05$; ** $p < 0.01$; *** $p < 0.001$.

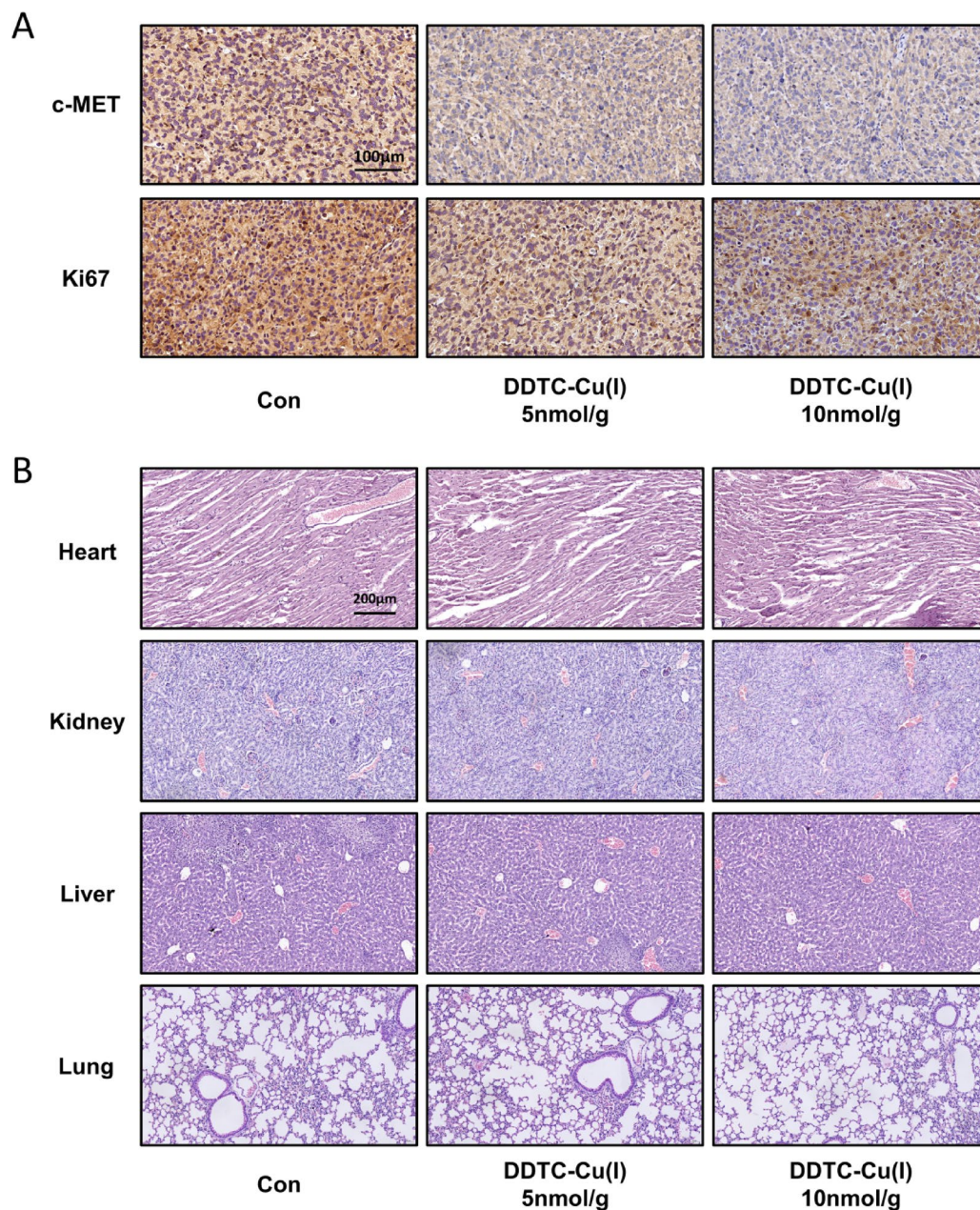


Fig. 8. (A) IHC staining of excised OS samples for c-MET and Ki67 protein level (scale bar, 200 μm). (B) H&E staining of heart, tumors, liver, kidney, and lungs samples (Scale bar, 200 μm).

Data availability

Data Availability Statement: The datasets used and/or analyzed during the current study are available from the corresponding author or public database. The experimental data of RNA-seq has been uploaded to the GEO database (accession number: GSE271220, <https://www.ncbi.nlm.nih.gov/geo/query/acc.cgi?acc=GSE271220>).

Received: 26 June 2024; Accepted: 10 June 2025

Published online: 01 July 2025

References

1. Mirabello, L., Troisi, R. J. & Savage, S. A. Osteosarcoma incidence and survival rates from 1973 to 2004: Data from the surveillance, epidemiology, and end results program. *Cancer* **115**, 1531–1543 (2009).
2. Luetke, A., Meyers, P. A., Lewis, I. & Juergens, H. Osteosarcoma treatment - where do we stand? A state of the art review. *Cancer Treat. Rev.* **40**, 523–532 (2014).
3. Durfee, R. A., Mohammed, M. & Luu, H. H. Review of osteosarcoma and current management. *Rheumatol. Ther.* **3**, 221–243 (2016).

4. Geller, D. S., Gorlick, R. & Osteosarcoma A review of diagnosis, management, and treatment strategies. *Clin. Adv. Hematol. Oncol.* **8**, 705–718 (2010).
5. Skrott, Z. et al. Alcohol-abuse drug disulfiram targets cancer via P97 segregase adaptor Npl4. *Nature* **552**, 194–199 (2017).
6. Li, H. et al. The combination of disulfiram and copper for cancer treatment. *Drug Discov Today* **25**, 1099–1108 (2020).
7. Mandell, J. B. et al. Aldh1a1 gene expression and cellular copper levels between low and highly metastatic osteosarcoma provide a case for novel repurposing with disulfiram and copper. *Sarcoma*. 1–12 (2022).
8. Guo, W. et al. The disulfiram/copper complex induces apoptosis and inhibits tumour growth in human osteosarcoma by activating the ros/jnk signalling pathway. *J. Biochem.* **170**, 275–287 (2021).
9. Chen, J. et al. The molecular mechanisms of copper metabolism and its roles in human diseases. *Pflugers Arch.* **472**, 1415–1429 (2020).
10. Han, J. et al. A binuclear complex constituted by diethyldithiocarbamate and copper(I) functions as a proteasome activity inhibitor in pancreatic cancer cultures and xenografts. *Toxicol. Appl. Pharmacol.* **273**, 477–483 (2013).
11. Zhang, G. et al. A multifunctional antibacterial coating on bone implants for osteosarcoma therapy and enhanced osteointegration. *Chem. Eng. J.* **428**, 131155 (2022).
12. Chen, C. et al. Mir-135a reduces osteosarcoma pulmonary metastasis by targeting both Bmi1 and Klf4. *Front. Oncol.* **11**, 620295 (2021).
13. Chen, C. L. et al. Mir-134 inhibits osteosarcoma cell invasion and metastasis through targeting Mmp1 and Mmp3 in vitro and in vivo. *Febs Lett.* **593**, 1089–1101 (2019).
14. Percie, D. S. N. et al. The arrive guidelines 2.0: Updated guidelines for reporting animal research. *PLoS Biol.* **18**, e3000410 (2020).
15. Kansara, M., Teng, M. W., Smyth, M. J. & Thomas, D. M. Translational biology of osteosarcoma. *Nat. Rev. Cancer* **14**, 722–735 (2014).
16. Gaspar, N. et al. Results of methotrexate-eposide-ifosfamide based regimen (M-Ei) in osteosarcoma patients included in the French Os2006/Sarcome-09 study. *Eur. J. Cancer.* **88**, 57–66 (2018).
17. Kanehisa, M., Furumichi, M., Sato, Y., Matsuura, Y. & Ishiguro-Watanabe, M. Kegg: Biological systems database as a model of the real world. *Nucleic Acids Res.* **53**, D672–D677 (2025).
18. Kanehisa, M., Goto, S. & Kegg Kyoto encyclopedia of genes and genomes. *Nucleic Acids Res.* **28**, 27–30 (2000).
19. Kanehisa, M. Toward understanding the origin and evolution of cellular organisms. *Protein Sci.* **28**, 1947–1951 (2019).
20. Yang, X., Liao, H. Y. & Zhang, H. H. Roles of met in human cancer. *Clin. Chim. Acta* **525**, 69–83 (2022).
21. Yang, X. P. et al. Pancreatic stellate cells increase pancreatic cancer cells invasion through the hepatocyte growth factor /C-Met/survivin regulated by P53/P21. *Exp. Cell. Res.* **357**, 79–87 (2017).
22. Wang, K., Zhuang, Y., Liu, C. & Li, Y. Inhibition of C-Met activation sensitizes osteosarcoma cells to cisplatin via suppression of the Pi3K-Akt signaling. *Arch. Biochem. Biophys.* **526**, 38–43 (2012).
23. Goetsch, L., Caussanel, V. & Corvaia, N. Biological significance and targeting of C-Met tyrosine kinase receptor in cancer. *Front. Biosci.* **18**, 454–473 (2013).
24. Guo, R. et al. Met-dependent solid tumours—molecular diagnosis and targeted therapy. *Nat. Rev. Clin. Oncol.* **17**, 569–587 (2020).
25. Wang, Q. et al. Mir-485-3P regulated by Malat1 inhibits osteosarcoma Glycolysis and metastasis by directly suppressing C-Met and Akt3/Mtor signalling. *Life Sci.* **268**, 118925 (2021).
26. Wen, J. et al. Macc1 contributes to the development of osteosarcoma through regulation of the Hgf/C-Met pathway and microtubule stability. *Front Cell. Dev. Biol* **8**(2020).
27. Fioramonti, M. et al. Cabozantinib affects osteosarcoma growth through a direct effect on tumor cells and modifications in bone microenvironment. *Sci Rep* **8** (2018).
28. Sampson, E. R. et al. The orally bioavailable met inhibitor PF-2341066 inhibits osteosarcoma growth and osteolysis/matrix production in a xenograft model. *J. Bone Min. Res.* **26**, 1283–1294 (2011).
29. Mei, L. et al. Norcantharidin inhibits proliferation and promotes apoptosis via C-Met/Akt/Mtor pathway in human osteosarcoma cells. *Cancer Sci.* **110**, 582–595 (2018).
30. Liu, H., Deng, H., Zhao, Y., Li, C. & Liang, Y. Lncrna Xist/Mir-34a Axis modulates the cell proliferation and tumor growth of thyroid Cancer through Met-Pi3K-Akt signaling. *J Exp. Clin. Cancer Res* **37** (2018).
31. Xu, J., Liu, S., Yang, X., Cao, S. & Zhou, Y. Paracrine Hgf promotes Emt and mediates the effects of Psc on chemoresistance by activating C-Met/Pi3K/Akt signaling in pancreatic cancer in vitro. *Life Sci.* **263**, 118523 (2020).
32. Sun, Z., Jian, Y., Zhu, H. & Li, B. Lncrapvt1 targets Mir-152 to enhance chemoresistance of osteosarcoma to gemcitabine through activating C-Met/Pi3K/Akt pathway. *Pathol. - Res. Pract.* **215**, 555–563 (2019).
33. Zhan, F. et al. Microrna-206 reduces osteosarcoma cell malignancy in vitro by targeting the Pax3-met axis. *Yonsei Med. J.* **60**, 163 (2019).
34. Polivka, J. J. & Janku, F. Molecular targets for cancer therapy in the Pi3K/Akt/Mtor pathway. *Pharmacol. Ther.* **142**, 164–175 (2014).
35. Yang, B. et al. Circular Rna circ_001422 promotes the progression and metastasis of osteosarcoma via the Mir-195-5P/Egf2/Pi3K/Akt axis. *J. Exp. Clin. Cancer Res.* **40**, 235 (2021).
36. Zhang, J., Yu, X. H., Yan, Y. G., Wang, C. & Wang, W. J. Pi3K/Akt signaling in osteosarcoma. *Clin. Chim. Acta.* **444**, 182–192 (2015).
37. Zhang, K., Wu, S., Wu, H., Liu, L. & Zhou, J. Effect of the Notch1-mediated Pi3K-Akt-Mtor pathway in human osteosarcoma. *Aging (Albany Ny)* **13**, 21090–21101 (2021).
38. Xiang, Y., Yang, Y., Liu, J. & Yang, X. Functional role of Microrna/Pi3K/Akt axis in osteosarcoma. *Front Oncol.* **13** (2023).

Author contributions

Author Contributions: Conceptualization, R.Z., L.Y. and X.S.; methodology, R.Z. and L.Y.; soft-ware, X.Q.; validation, K.Z., S.C. and Y.Y.; formal analysis, Y.P.; investigation, C.X.; resources, X.W., Z.T. and Y.F.; data curation, R.Z.; writing original draft preparation, R.Z.; writing—review and editing, L.Y.; visualization, R.Z.; supervision, Z.L.; project administration, P.L.; funding acquisition, Z.T. and Y.F. All authors have read and agreed to the published version of the manuscript.

Funding

This research was funded by the National Natural Science Foundation of China: U21A20353; National Natural Science Foundation of China: 82172503; National Natural Science Youth Fund: 82302769; National Science Foundation of Shanxi Province [20210302123263; 20210302124410; 20210302124419; 202204041101023], The Second Hospital of Shanxi Medical University, and four research funding projects within the hospital [2020001-10].

Declarations

Competing interests

The authors declare no competing interests.

Additional information

Supplementary Information The online version contains supplementary material available at <https://doi.org/10.1038/s41598-025-06748-6>.

Correspondence and requests for materials should be addressed to Y.F. or Z.T.

Reprints and permissions information is available at www.nature.com/reprints.

Publisher's note Springer Nature remains neutral with regard to jurisdictional claims in published maps and institutional affiliations.

Open Access This article is licensed under a Creative Commons Attribution-NonCommercial-NoDerivatives 4.0 International License, which permits any non-commercial use, sharing, distribution and reproduction in any medium or format, as long as you give appropriate credit to the original author(s) and the source, provide a link to the Creative Commons licence, and indicate if you modified the licensed material. You do not have permission under this licence to share adapted material derived from this article or parts of it. The images or other third party material in this article are included in the article's Creative Commons licence, unless indicated otherwise in a credit line to the material. If material is not included in the article's Creative Commons licence and your intended use is not permitted by statutory regulation or exceeds the permitted use, you will need to obtain permission directly from the copyright holder. To view a copy of this licence, visit <http://creativecommons.org/licenses/by-nc-nd/4.0/>.

© The Author(s) 2025